



Wind Energy Conversion System Oscillations Damping Using a Proposed Mutation Operator for LBBO-DE Algorithm

Tarek Boghdady, Mahmoud Sayed and Howaida M. Ragab

EasyChair preprints are intended for rapid dissemination of research results and are integrated with the rest of EasyChair.

December 1, 2019

Wind Energy Conversion System Oscillations Damping Using a Proposed Mutation Operator for LBBO-DE Algorithm

T. A. Boghdady

*Electric Power Engineering Dept.,
Cairo University
Giza, , Egypt.
engtarek82@gmail.com*

M. M. Sayed

*Electric Power Engineering Dept.,
Cairo University
Giza, , Egypt.
fecu.msayed@gmail.com*

Howaida M. Ragab

*Electric Power Engineering Dept.,
Ahram Canadian University of
Giza, Egypt.
enghowaida@yahoo.com*

Abstract— Damping the oscillations of the wind energy conversion system of a grid connected Doubly Fed Induction Generator (DFIG) is the main objective in this article. PID controller is commonly used in many industrial process, but its parameter tuning is a challenging task. The PID parameters values are not optimally adjusted by conventional methods being used such as frequency response. Such that, a new algorithm is used which is hybrid Differential Evolution with Linearized Biogeography-Based Optimization (LBBO-DE). Linearized-Biogeography Based Optimization (LBBO) is a new version of Biogeography-Based Optimization (BBO). Cauchy and Gaussian mutation operators are proposed to modify the mutation equation. The algorithm LBBO-DE with the proposed mutation operators had been tested with 53 benchmarks and then compared with the 40 algorithms that have been accepted for 2005 and 2011 Congress on Evolutionary Computation (CEC). The proposed algorithm achieved advanced rank between them and gave better results and lower variance, which proved to have competitive performance with state-of-the-art evolutionary algorithms. A simulation model is used to show the oscillation damping in case of symmetrical and asymmetrical fault occurrence at the grid connected to WECS-DFIG. As a result, the LBBO-DE with Gaussian mutation equation is used to optimize the controller parameters for achieving oscillations damping. The simulation results of direct-drive PMSG model is also used for the oscillations damping purpose under the case of wind speed variation, which is done by the LBBO-DE.

Keywords— *Doubly Fed Induction Generator, Permanent magnet synchronous generator, Optimization, Wind energy conversion system.*

I. INTRODUCTION

Developing wind energy generation has an increasing interest in the last decade. A lot of objectives can be achieved by using electrical controller especially in variable speed operations as wind energy systems [1-3]. Finding the parameters of PID and PI controllers is a challenging task. PID parameters can not often be tuned at their optimum values due to the difficulties of the conventional techniques that are being used such as frequency response. But, today intelligent control has become a focus of research as Artificial Neural Network (ANN) controller, fuzzy controller, and evolutionary algorithms based controller [4].

In the last few decades, Evolutionary Algorithms (EAs) proved their effectiveness as an optimization tool. EAs are often based on mathematics of a natural process in which EA attempts to emulate the nature of some organisms in its

method of selection as Genetic Algorithm (GA), Particle Swarm Optimization (PSO), Ant Colony Optimization (ACO), and Differential Evolution (DE).

The rest of the paper is organized as follows: section 2 introduces a brief about the optimal control of wind turbines. Section 3 proposes the Gaussian and Cauchy operators that will be applied to LBBO-DE, then a comparison with the algorithms that being used in 2005 and 2011 Congress of Evolutionary Computation (CEC). Section 4 simulates a laboratory prototype of a WECS-DFIG under symmetrical and asymmetrical fault conditions. Another test of wind speed variation is simulated and discussed in section 5. Finally, the conclusions are summarized in section 6.

II. OPTIMAL CONTROL OF WIND TURBINES

In this section many optimization methods, is used in researches, will be discussed. In [5] an optimal neural network sliding mode control based on adaptive PSO algorithm for maximization of power and minimization of shaft stresses. The neural network is used here to estimate the uncertain parts of the system, but it is assumed to have ideal gear ratio. In [6] the adaptive SMES controller was tuned using improved PSO to get the learning data for radial basis function neural network, the objective function is shown in equation (1)

$$J_{obj} = \sum_{i=1}^N (\xi(i) - \xi_0)^2 \quad (1)$$

where ξ_0 is the desired damping ratio. In paper [7] the objective function is slightly changed from equation (1), as the author is interested not only the damping ratio but also the settling time as shown in equation (2)

$$J_{obj} = \sum_{i=1}^N |\xi(i) - \xi_0| + \sum_{i=1}^N |\sigma(i) - \sigma_0| \quad (2)$$

where σ_0 is the desired real part of the desired eigenvalues.

In [8] a comparative study for PI tuning was done using self-adaptive global best harmony search, simulated annealing, bees' colony, and Ziegler-Nichols technique. The objective function was the integral of absolute error, which is the difference between the measured and the reference current values.

Paper [9] presents a PSO method for determining the parameters of PI controller for PMSG to improve the control ability. The aim here is to optimize the parameters of PI controllers of the generator-side converter which is used to

control the dc-link voltage and the grid-side converter which is responsible for the control of power flow injected into the grid using the algorithm (LBBO-DE) [10].

One important rule is that the WECS should be able to stay operating during grid disturbances or faults and provide ancillary services in order to support the utility.

III. MUTATION EQUATION

The mutation operator is one of the main operators in Evolutionary Algorithms (EA) [11] so it is frequently used in EAs [12- 13]. The new offspring that is obtained by recombination only will be in the neighborhood from the first generation. So EAs can improve their quality in solution by using a mutation strategy. There are a lot of mutation operators in EAs, for example, Cauchy mutation [11], Gaussian mutation [11], Lévy mutation [13], exponential mutation [14], t mutation [15], and mix mutation strategy [16].

The first two strategies will be used for two reasons: First, is that methods are successfully widely used in EAs. Second, the two methods are able to perform either local search or global search depending on the step size used. Mutation operators improve the diversity of population especially in the early and middle stages of the EAs [17].

1. Cauchy Mutation

The Cauchy distribution has the following probability density function [18]

$$f_t(x) = \frac{1}{\pi} \frac{t}{t^2 + x^2} \quad (3)$$

where $x \in \mathbb{R}$ and $t > 0$ is a scale parameter. A real-valued random variable Y is indicated to be Cauchy distributed with $t > 0$, it can be written as:

$$Y \sim \delta(t)$$

The Cauchy mutation with $t = 1$ can be described as [11]

$$X'_i(j) = X_i(j) + \delta_j(1) \quad (4)$$

2. Gaussian Mutation

The probability density function of the Gaussian distribution [18] is

$$f_{\mu, \sigma^2}(x) = \frac{1}{\sigma\sqrt{2\pi}} e^{-\frac{(x-M)^2}{2\sigma^2}} \quad (5)$$

where M is the mean and σ^2 is the variance. To indicate that a real-valued random variable Y is normally distributed with mean μ and variance $\sigma^2 \geq 0$, it can be written as:

$$Y \sim N(M, \sigma^2)$$

Then the Gaussian mutation with $M = 0$ and $\sigma = 1$ can be described as:

$$X'_i(j) = X_i(j) + N_j(0,1) \quad (6)$$

where $X_i(j)$ is the j th decision variable of individual X_i and $N_j(0, 1)$ indicates that the random number is generated a new for each value of j .

A. Benchmark problems from the 2005 CEC

The modified LBBO-DE method is tested with 25 benchmark functions from the 2005 CEC (F1-F25). Each simulation was limited to 10,000D function evaluations (FEs), where D is the problem dimension. A mutation probability of 0.01 and a population size of 50 were used, we run 100 independent Monte Carlo simulations for each function using MATLAB software [19].

Table I shows the results of LBBO-DE, the modified LBBO-DE with Cauchy mutation operator (LBBO-DE-C), and the modified LBBO-DE with Gaussian mutation operator (LBBO-DE-G), the mean value, standard deviation, and the minimum value are the three factors that had been selected for this comparison for 2005 CEC. If the obtained value for LBBO-DE-C or LBBO-DE-G was smaller or equal the rival value obtained with LBBO-DE, this value will be shown with grey background.

TABLE I. MEAN, STANDARD DEVIATION AND MINIMUM VALUES OBTAINED BY LBBO-DE, LBBO-DE-C AND LBBO-DE-G AFTER SIMULATION FOR 2005 CEC

Bench Marks	LBBO-DE			LBBO-DE-C			LBBO-DE-G		
	Mean	Std.	Min.	Mean	Std.	Min.	Mean	Std.	Min.
F1	0	0	0	0	0	0	0	0	0
F2	0	0	0	0	0	0	0	0	0
F3	0	0	0	6.14E-14	6.14E-13	0	0	0	0
F4	896.1412	549.801	23.7965	738.384	4.79E+02	32.34714	735.9662	507.324503	26.57981
F5	0.003569698	0.005115135	5.74E-07	0.003234	0.00486787	6.4E-07	0.003349	0.00465219	6.43E-07
F6	0.000214	0.001027337	2.58E-10	0.000303	0.001452546	2.82E-10	0.000268	0.00139426	1.45E-10
F7	0.064710636	0.176131622	2.15E-10	0.094212	0.219690259	6.43E-11	0.081718	0.21967836	1.58E-10
F8	20	5.56E-14	20	20	0	20	20	0	20
F9	1.66E-11	1.72E-11	5.68E-13	1.37E-11	1.58E-11	6.25E-13	1.06E-11	1.26E-11	1.14E-13
F10	12.93445489	3.880601908	5.969754	13.19314	4.058494845	4.974795	13.22299	3.68850368	4.974795
F11	5.407172386	1.135255189	2.483088	5.204084	1.104829291	2.083162	5.186918	0.98780352	1.971617
F12	0.012760872	0.099094947	1.05E-10	0.014011	0.091685573	2.94E-10	0.029686	0.13702696	5.45E-11
F13	0.397148895	0.121280175	0.099567	0.426065	0.162580409	0.069499	0.412454	0.14725291	0.039756
F14	3.151259071	0.443453876	1.988146	3.245726	0.466986328	1.811717	3.220568	0.46906044	1.546704
F15	2.106583543	21.06583543	1.42E-14	1.49E-12	1.55E-12	1.42E-14	1.56E-12	1.58E-12	0
F16	121.6195354	12.8259731	85.24898	122.5691	14.37702146	93.21139	124.2536	12.6694103	97.14865
F17	156.3706808	18.77672062	105.8451	151.917	19.35921799	91.0101	152.3154	15.8681661	112.6201
F18	739.5007312	148.1771848	353.8454	712.1436	159.342567	300	717.8048	153.880196	354.9766
F19	734.5556789	147.9724779	377.3104	726.7924	169.012359	300	730.6912	155.289419	300
F20	733.2950542	151.6700225	300	713.1218	153.982001	353.8628	726.8401	140.826426	356.3574
F21	514.0304474	227.1642503	200	497.0747	194	200	465.3955	170.853925	200
F22	699.9683164	186.9898363	300	711.1762	175.542390	300	700.5269	184.883485	300
F23	635.9960656	123.1688574	425.1725	626.2779	102	425.1725	621.0452	82.4685236	425.1725
F24	205.4350093	3.98150598	200.2898	205.2247	3.312273914	200.3992	205	3.73358533	200
F25	205.5346597	4.006521959	200.4213	205.6042	4.693435759	200.8423	206	4.20556783	200

Form Table I, it can be concluded that Gaussian mutation gives better results than Cauchy mutation as it gives minimum value for 19 benchmark functions while Cauchy mutation gives minimum value for 16 benchmark functions, also for the mean value of 100 independent runs Gaussian mutation improved in 17 benchmark functions compared to LBBO results, while Cauchy mutation improved in 15 benchmark functions, finally, for the standard deviation Gaussian mutation improved in 17 benchmark functions compared to LBBO-DE results, while Cauchy mutation improved in 13 benchmark.

B. Benchmark problems from the 2011 CEC

The modified LBBO-DE method is tested with the 22 real-world benchmark functions from the 2011 CEC [20-21].

Each simulation is limited to 150,000 function evaluations as in the 2011 CEC. The parameters are adjusted to be the same as used before with benchmarks stated in 2005 CEC. For more information about the benchmark functions, read [22].

Table II shows the results of LBBO-DE, LBBO-DE-C, and LBBO-DE-G, the mean value, standard deviation, and the minimum value are the three factors that had been selected for this comparison for 2011 CEC. If the obtained value for LBBO-DE-C or LBBO-DE-G was smaller or equal the rival value obtained with LBBO-DE, this value will be written with grey background.

TABLE II. MEAN, STANDARD DEVIATION, AND MINIMUM VALUES OBTAINED BY LBBO-DE, LBBO-DE-C AND LBBO-DE-G AFTER SIMULATION FOR 2011 CEC

Bench Marks	LBBO-DE			LBBO-DE-C			LBBO-DE-G		
	Mean	Std.	Min.	Mean	Std.	Min.	Mean	Std.	Min.
T1	5.374897371	5.812159453	0	5.43973	6.056701752	2.00E-15	5.43973	6.05670175	2.00E-15
T2	-27.1176974	0.785737018	-28.4225	-27.2204	1.545896223	-28.4225	-27.2204	1.54589622	-28.4225
T3	1.15E-05	8.51E-21	1.15E-05	1.15E-05	8.51E-21	1.15E-05	1.15E-05	8.51E-21	1.15E-05
T4	13.85788852	0.053737385	13.77134	13.85509	0.043848034	13.77327	13.86565	0.04478182	13.77215
T5	-35.8576523	1.001360268	-36.9165	-36.0386	0.869109018	-36.9157	-36.0356	0.99014226	-36.9147
T6	-27.046132	2.53814761	-29.1661	-27.1837	2.296753748	-29.1661	-27.0616	2.32885416	-29.1661
T7	0.822671771	0.107608775	0.5	0.816632	0.106132563	0.54785	0.799672	0.10541434	0.5
T8	220	0	220	220	0	220	220	0	220
T9	4.80E+04	1.90E+04	1.74E+04	46944.54	16964.12793	16147.06	4.99E+04	1.76E+04	1.93E+04
T10	-14.6124474	2.729473214	-20.9259	-14.6291	2.618689718	-21.2596	-14.6157	3.03630378	-20.8718
T11.1	52055.80287	442.074931	50798.43	5.21E+04	3.46E+02	5.12E+04	5.21E+04	4.40E+02	5.13E+04
T11.2	19433759.02	302739.4378	18821209	1.95E+07	2.92E+05	1.90E+07	1.95E+07	3.43E+05	1.87E+07
T11.3	15450.55923	2.995139965	15444.54	1.55E+04	2.984692209	1.54E+04	1.55E+04	2.66038994	1.54E+04
T11.4	18307.77368	71.13121598	18146.98	1.83E+04	64.45305836	1.82E+04	1.83E+04	61.9845422	1.82E+04
T11.5	3.29E+04	53.55355043	3.28E+04	3.29E+04	45.43298502	3.28E+04	3.29E+04	43.1276185	3.28E+04
T11.6	1.40E+05	3.13E+03	1.34E+05	1.40E+05	3.65E+03	1.32E+05	1.40E+05	3.37E+03	1.33E+05
T11.7	1.76E+07	1.49E+07	1.96E+06	1.92E+07	1.31E+07	2.19E+06	1.69E+07	1.39E+07	2.03E+06
T11.8	1.87E+06	6.11E+05	1.14E+06	1.85E+06	5.41E+05	1.20E+06	2.01E+06	1.42E+06	1.10E+06
T11.9	2.26E+06	8.55E+05	1.43E+06	2.24E+06	5.56E+05	1.31E+06	2.25E+06	1.06E+06	1.17E+06
T11.10	2.02E+06	1.09E+06	1.09E+06	1.89E+06	6.54E+05	1.10E+06	2.00E+06	1.49E+06	1.23E+06
T12	16.16386281	2.178779387	9.835944	16.08263	2.176043232	7.838117	15.80782	2.09822799	8.595823
T13	19.82948251	3.086162818	11.4368	20.49156	3.011346024	11.25705	19.71734	2.82062905	11.28336

Form Table II, Gaussian mutation gives minimum value for 12 benchmark functions from 2011 CEC functions while Cauchy mutation gives minimum value for 10, but for the mean value of 100 independent runs Gaussian mutation improved in 15 benchmark functions compared to LBBO-DE results, while Cauchy mutation improved in 16 benchmark functions, finally, for the standard deviation Gaussian mutation improved in 14 benchmark functions compared to LBBO results, while Cauchy mutation improved in 19 benchmark functions.

It can be noticed that Gaussian mutation operator gives better results than Cauchy mutation operator in its minimum, mean, and standard deviation values for the 2005 CEC on 25 benchmark problems, but for 2011 CEC on 22 benchmark problems Gaussian mutation operator gives better results in the minimum values while Cauchy mutation operator gives better results in the benchmarks functions' mean and standard deviations values.

IV. WECS-DFIG SUBJECTED TO FAULT

In the case of grid faults, there is a power mismatch between the generated active power and the active power delivered to the grid, which it will lead to accelerate the generator speed.

It can be noticed, from Figures 1 and 2, that the system retrieves its steady state values faster (i.e. smaller settling time) with lower maximum percent of overshoot and maximum percent undershoot for the controller parameters based on the LBBO-DE with Gaussian mutation compared to the values obtained using GA.

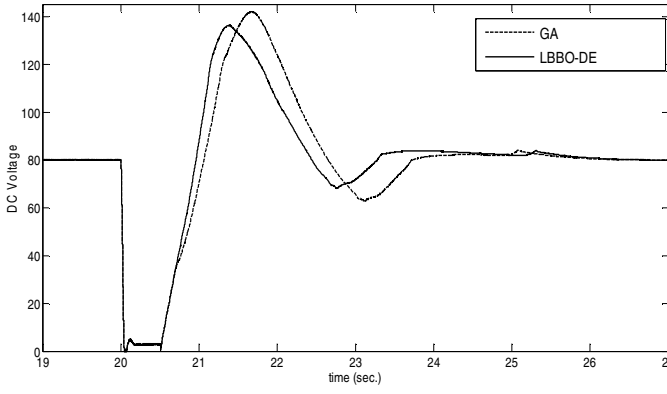


Fig. 1. The DC voltage (v.) response obtained using GA and LBBO-DE with Gaussian mutation after the three phase to ground fault occurrence.

From Fig. 1, it can be noticed that the maximum percent undershoot is 2.5% for the LBBO-DE-G with settling time of 2.9 sec., while the maximum percent undershoot obtained with the GA is 7.5% with settling time of 3.4 sec.

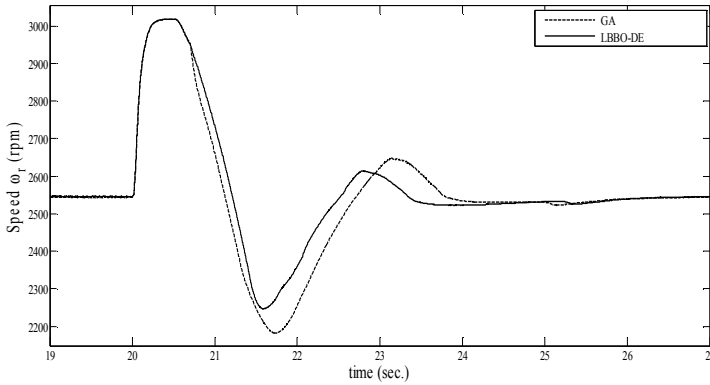


Fig. 2. The rotor speed (ω_r) response obtained using GA and LBBO-DE with Gaussian mutation after the three phase to ground fault occurrence.

Figure 2 shows that there is an overshoot with 2.75% for the LBBO-DE with Gaussian mutation algorithm-based controller, while the overshoot percent obtained using the GA is 4.31%. also, the maximum percent undershoot obtained by the LBBO-DE-G algorithm is 7.84%, while its rival values obtained by the GA is 14.51%. The system is faster as it has smaller settling time of 3.4 sec., while the GA gave slower response with settling time value of 4.4 sec.

Asymmetrical grid faults such as single line to ground happen more often than the symmetrical faults. During the asymmetrical grid fault, there will be a negative-sequence voltage, which can lead to second-order harmonics in the injected currents that affects on the DC link voltage.

A single phase to ground fault is implemented via the simulation using (MATLAB/SIMULINK). The fault occurs at the instant of 20 sec. from the simulation starting and it lasts for 0.5 sec. as shown in Figures 3 and 4.

Figure 3 shows the DC link voltage after the single phase to ground fault occurrence. During the asymmetrical fault there is a high frequency ripples in the DC link voltage profile due to the existence of negative sequence. After the fault clearance, both DC link voltage profiles retrieve their initial value of 80 v. but the DC voltage obtained using LBBO-DE with Gaussian mutation has better performance (i.e. lower overshoot and faster settling time). It can be noticed that the maximum percent undershoot is 11.37% for the LBBO-DE with settling time of 1.64 sec., while the maximum percent

undershoot obtained with the GA is 15.65% with settling time of 1.84 sec.

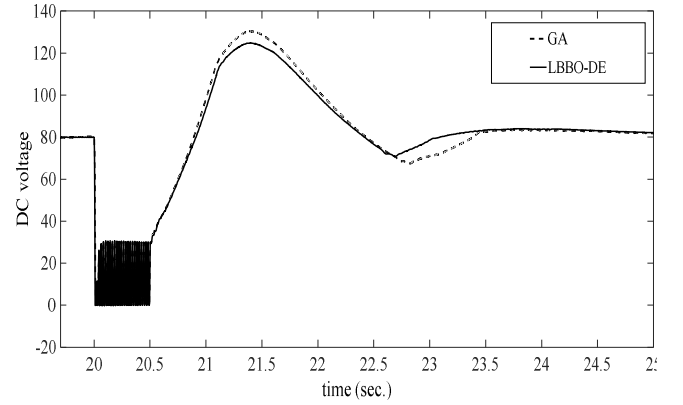


Fig. 3. The DC voltage (v.) response obtained using GA and LBBO-DE with Gaussian mutation after the single line to ground fault occurrence.

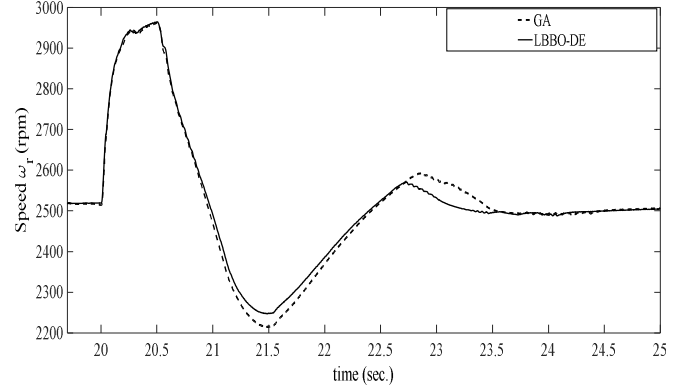


Fig. 4. The rotor speed (ω_r) response obtained using GA and LBBO-DE with Gaussian mutation after the single phase to ground fault.

Figure 4 shows the speed after the single phase to ground fault. There is an overshoot with 1.9% for the profile obtained by the LBBO-DE algorithm based controller, while the overshoot percent obtained using the rival GA is 3.1%. also, the maximum percent undershoot obtained by the LBBO-DE algorithm is 10.6%, while its rival values obtained by the GA is 11.92%. The system is faster as it has smaller settling time of 1.61 sec., while the GA gave slower response with settling time of 2 sec. The high speed frequency of the negative sequence, resulted in asymmetrical fault, do not have the same effect as in DC link voltage profile as the mechanical system is usually slower than the electrical system.

V. PMSG WIND TURBINE SYSTEM

A direct-drive PMSG wind turbine is depicted in Fig. 5. The generated power by the PMSG is fed to the grid through a variable-frequency converter, which consists of a generator-side converter and a grid-side converter connected back-to-back via a DC link.

A. Modeling of the Wind Turbine

The power coefficient (C_p) is a function of the tip-speed ratio (λ) and the pitch angle (β), C_p for both fixed and variable speed wind turbines is computed based on the turbine characteristics in reference [23] by:

$$C_p = C_1 \left(C_2 \left(\frac{1}{\lambda + 0.08\beta} - \frac{0.035}{\beta^3 + 1} \right) - C_3\beta - C_4 \right) e^{-C_5 \left(\frac{1}{\lambda + 0.08\beta} - \frac{0.035}{\beta^3 + 1} \right)} + C_6\lambda \quad (7)$$

where C_1 to C_6 are [0.5176, 116, 0.4, 5, 21, 0.0068]. The peak value of C_p is obtained at $\beta = 0^\circ$ and λ_{opt} .

B. Modeling of PMSG

The PMSG equations are given in d-q frame as [24]:

$$v_{ds} = R_s i_{ds} + L_{ds} \frac{di_{ds}}{dt} - \omega_r L_{qs} i_{qs} \quad (8)$$

$$v_{qs} = R_s i_{qs} + L_{qs} \frac{di_{qs}}{dt} + \omega_r L_{ds} i_{ds} + \omega_r \psi_f \quad (9)$$

$$T_e = p(\psi_f i_{qs} + (L_{ds} - L_{qs}) i_{ds} i_{qs}) \quad (10)$$

Where v_{ds} and v_{qs} are the direct and quadrature components of the stator voltage, R_s is the stator resistance, i_{ds} and i_{qs} are the direct and quadrature components of the stator currents, L_{ds} and L_{qs} are the direct and quadrature components of the stator self inductance, ω_r is the electrical angular speed, and ψ_f is the permanent magnet rotor magnetic flux, while the grid voltage are given in the (d-q) frame that is rotating with the angular frequency ω by:

$$v_d = R_{gf} i_d + L_d \frac{di_d}{dt} - L_q i_q + E_s \quad (11)$$

$$v_q = R_{gf} i_q + L_q \frac{di_q}{dt} + \omega L_d i_d \quad (12)$$

where R_{gf} is the filter resistance which is located between the grid side converter and the grid, i_d and i_q are the direct and quadrature components of the grid side converter output currents, L_d and L_q are the direct and quadrature components of the filter inductance, and E_s is the maximum grid phase voltage.

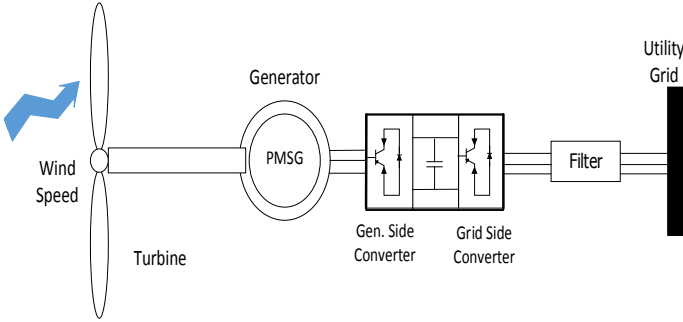


Fig. 5. PMSG wind energy system.

C. Generator Side Converter Control

Its objective is to control the speed of the PMSG by using Field oriented control (FOC) to achieve variable speed operation with MPPT control. This controller requires 3 PI controllers, one controller for the rotor speed while the others for the d-q. Maximum Torque per Ampere control strategy is used to control the d and q-axis currents.

D. Grid Side Converter Control

Its objective to control both of the DC bus voltage (V_{dc}) and the reactive power transmitted to the grid. Also, FOC controller is applied to the grid side converter. This controller requires 4 PI controllers, two for the currents while the others for the reactive power and DC link voltage.

Simulation is carried out using MATLAB/SIMULINK for 1.5 MW PMSG wind turbine, the per unit (pu) values of the WECS-PMSG stated in [25]. The per unit values are:

$$I_b = \frac{P_b}{3V_b}, \omega_b = 2\pi f_b, \omega_{bm} = \frac{\omega_b}{P}, L_b = \frac{Z_b}{\omega_b}, C_b = \frac{1}{\omega_b Z_b},$$

$$T_b = \frac{P_b}{\omega_{bm}}, J_b = \frac{2P_b P^2}{\omega_b^2}, K_b = \frac{2P_b P^2}{\omega_b}, \psi_{rb} = \frac{\sqrt{2}V_b}{\omega_b}$$

Where the subscript ‘‘b’’ means the base value of this quantity; I, V, P, f are the current, voltage, power, and frequency, respectively; Z, L, C are the impedance, inductance and capacitance, respectively; ω , ω_m are the electrical and mechanical angular frequencies, respectively; T is the torque; J, K are the inertia and stiffness, respectively; p is the number of pair poles pairs; and ψ_r is the amplitude of the rotor flux. The parameters of the WECS-PMSG are listed in Table III.

The applied wind speed is changed from 10 m/sec. to 12 m/sec. after 10 sec. from the simulation starting, and then it is decreased to 8 m/sec. after 20 sec. from the simulation starting. The DC voltage is set at 1500 v. The simulation results for the PMSG using PI controllers optimized by the LBBO-DE-G is compared to the GA. The PI gains of the current controllers of the converters have the same values. The objective functions is given by equation (13).

$$J_{obj} = \int (v_{dc_{ref}} - v_{dc})^2 dt + \int (\omega_{r_{ref}} - \omega_r)^2 dt \quad (13)$$

Where $v_{dc_{ref}}$ is the reference value for the DC link voltage and $\omega_{r_{ref}}$ is the reference for the electrical angular speed.

TABLE III. THE WECS-PMSG PARAMETERS

Base power P_b (MVA)	1.5	Base voltage V_b (V)	$690/\sqrt{3}$
Rated generator speed (pu)	1	Rated generator line voltage	1
Base frequency f_b (Hz)	11.5	Inertia of PMSG (pu)	0.5
Number of pair poles P	40	Shaft stiffness (pu)	2
Nominal wind turbine mechanical power (pu)	1.1	Generator inductance in the q-frame (pu)	0.7
Nominal wind turbine speed (pu)	1.2	Generator stator resistance (pu)	0.01
Generator inductance in the direct frame (pu)	0.7	Flux of the permanent magnets (pu)	0.9
Inertia of the wind turbine (pu)	4.8	DC-link capacitance (pu)	1
Rate wind speed (m/s)	12	Line inductance (pu)	0.1
Rated generator torque (pu)	1	Rated generator power (pu)	1

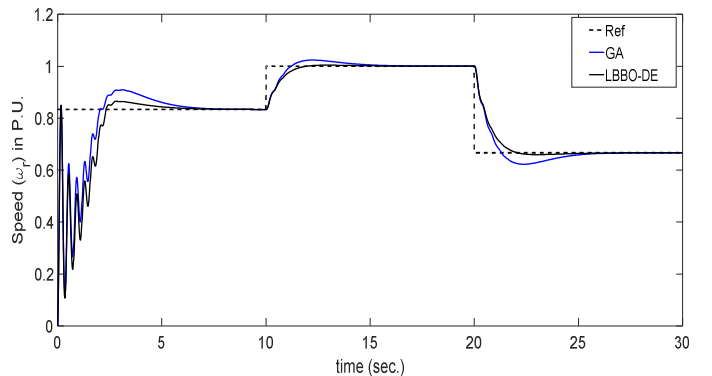


Fig. 6. The rotor speed (ω_r), in per unit, response obtained using GA and LBBO-DE with Gaussian mutation.

Figure 6 shows the rotor speed profile in (rpm). It can be noticed from Fig. 6 that the speed response obtained with LBBO-DE has a smaller overshoot of 0.48 % with faster settling time of 4.05 sec. when it is compared to GA, which

has an overshoot of 2.36 % and settling time of 5.75 sec. for the undershoot which occurred after the instant of 20 sec., it can be noticed that the maximum percent undershoot, obtained using the LBBO-DE-G, is smaller (1.09%) than the value obtained using GA (6.61%), also with a faster settling time.

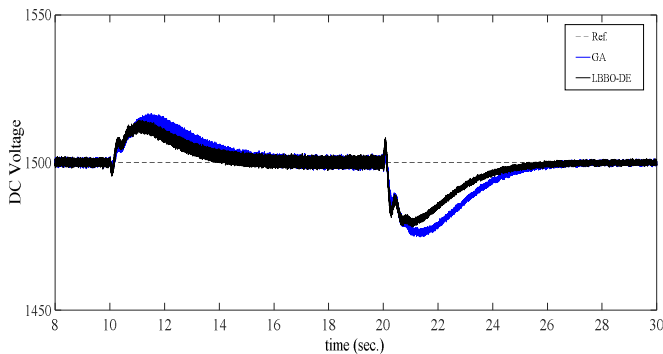


Fig. 7. The DC voltage (v.) response obtained using GA and LBBO-DE with Gaussian mutation.

From Fig. 7, The DC link settles faster using the LBBO-DE-G with 4.03 sec. Also, with smaller overshoot of 0.87% than with GA with overshoot of 1.11% and settling time of 4.58 sec. For the instant of undershoot occurrence, it can be noticed that the maximum percent undershoot, obtained using the LBBO-DE, is smaller and faster in its settling time, if it compared with the rival values obtained with GA. The less maximum overshoot and settling time responses of the generator speed and DC link voltage for LBBO-DE improves the low voltage ride through capability of the PMSG wind system.

VI. CONCLUSIONS

The LBBO-DE algorithm with Cauchy and Gaussian mutation operators is introduced to reduce the rotational variance of LBBO-DE. This modified version of LBBO-DE had been compared with the original LBBO-DE with the 2005 CEC on 25 benchmark problems and also compared to the 2011 CEC on 22 real-world problems. The results show that LBBO-DE-G gives minimum value (the best) for 31 bench marks (19 in 2005 and 12 in 2011) while LBBO-DE-C gives minimum value (the best) for 26 bench marks (16 in 2005 and 10 in 2011). For the average values, also LBBO-DE-G gives better results than the LBBO in 32 bench marks while LBBO-DE-C gives better results than the LBBO-DE in 31 bench marks. So that, the Gaussian mutation operator is selected to be the mutation operator being used.

the oscillations damping, is achieved in speed variation disturbance for PMSG. Also, the oscillations damping is achieved in the symmetrical three phase fault case and in the asymmetrical single line to ground fault for the DFIG.

REFERENCES

- [1] Spée, René, Shibashis Bhowmik, and Johan HR Enslin. "Novel control strategies for variable-speed doubly fed wind power generation systems." *Renewable Energy* 6.8 (1995): 907-915.
- [2] Novak, Peter, et al. "Modeling and control of variable-speed wind-turbine drive-system dynamics." *Control Systems, IEEE* 15.4 (1995): 28-38.
- [3] Valenciaga, F., P. F. Puleston, and Sarah K. Spurgeon. "A geometric approach for the design of MIMO sliding controllers. Application to a wind-driven doubly fed induction generator." *International Journal of Robust and Nonlinear Control* 19.1 (2009): 22-39.

- [4] Jabban, Taha Muhamad, et al. "Enhancing the step response curve for rectifier current of HVDC system based on artificial neural network controller." *Journal of King Saud University-Engineering Sciences* 24.2 (2012): 181-192.
- [5] Boufounas, El-mahjoub, Jaouad Boumhidi, and Ismail Boumhidi. "Optimal neural network sliding mode control for a variable speed wind turbine based on APSO algorithm." *2014 Second World Conference on Complex Systems (WCCS), IEEE, Agadir, Morocco, Nov. 2014.*
- [6] Rahim, A. H. M. A., and Muhammad Haris Khan. "An adaptive optimum SMES controller for a PMSG wind generation system." *Power and Energy Society General Meeting (PES), IEEE, 2013.*
- [7] Ngamroo, Issarachai, et al. "Power oscillation suppression by robust SMES in power system with large wind power penetration." *Physica C: Superconductivity* 469.1 (2009): 44-51.
- [8] Ali, Ahmad, et al. "Comparative performance of wind turbine driven PMSG with PI-controllers tuned using heuristic optimization algorithms." *International Energy Conference (ENERGYCON), IEEE, 2014.*
- [9] Sun, Lixia, and Chengya Gong. "Design and optimization of control parameters based on direct-drive permanent magnet synchronous generator for wind power system." *8th Conference on Industrial Electronics and Applications (ICIEA), IEEE, 2013.*
- [10] Boghdady, T. A., M. M. Sayed, and EE Abu Elzhab. "Maximization of generated power from wind energy conversion system using a new evolutionary algorithm." *Renewable energy* 99 (2016): 631-646.
- [11] Yao, Xin, Yong Liu, and Guangming Lin. "Evolutionary programming made faster." *IEEE Transactions on Evolutionary Computation*, 3.2 (1999): 82-102.
- [12] Yang, Zhenyu, Xin Yao, and Jingsong He. "Making a difference to differential evolution." *Advances in metaheuristics for hard optimization. Springer Berlin Heidelberg, 2007.* 397-414.
- [13] Lee, Chang-Yong, and Xin Yao. "Evolutionary programming using mutations based on the Lévy probability distribution." *IEEE Transactions on Evolutionary Computation*, 8.1 (2004): 1-13.
- [14] Narihisa, H., et al. "Evolutionary programming with exponential mutation." *Proceedings of the IASTED artificial intelligence and soft computing, Benidorn, Spain (2005):* 50-55.
- [15] Gong, Wenyin, et al. "A new mutation operator based on the T probability distribution in evolutionary programming." *5th International Conference on Cognitive Informatics, ICCI, Vol. 2. IEEE, 2006.*
- [16] Dong, Hongbin, et al. "Evolutionary programming using a mixed mutation strategy." *Information Sciences* 177.1 (2007): 312-327.
- [17] Gong, Wenyin, et al. "A real-coded biogeography-based optimization with mutation." *Applied Mathematics and Computation* 216.9 (2010): 2749-2758.
- [18] Feller, William. *An introduction to probability theory and its applications. Vol. 2. John Wiley & Sons, 2008.*
- [19] Suganthan, Ponnuthurai N., et al. "Problem definitions and evaluation criteria for the CEC 2005 special session on real-parameter optimization." *Technical Report, Nanyang Technological University, Singapore, 2005.*
- [20] Simon, Dan, Mahamed GH Omran, and Maurice Clerc. "Linearized biogeography-based optimization with re-initialization and local search." *Information Sciences* 267 (2014): 140-157.
- [21] Das, S. Suganthan, P. "Problem definitions and evaluation criteria for CEC 2011 competition on testing evolutionary algorithms on real world optimization problems." *Technical Report, Jadavpur University, Nanyang Technological University, 2010.*
- [22] Suganthan, P. "Competition on testing evolutionary algorithms on real-world numerical optimization problems at CEC2011." *New Orleans, USA, June 2011.*
- [23] Heier, Siegfried. *Grid integration of wind energy conversion systems. Wiley, 1998.*
- [24] Foo, Gilbert, and M. F. Rahman. "Sensorless direct torque and flux-controlled IPM synchronous motor drive at very low speed without signal injection." *IEEE Transactions on Industrial Electronics*, 57.1 (2010): 395-403.
- [25] Geng, Hua, et al. "Unified power control for PMSG-based WECS operating under different grid conditions." *IEEE Transactions on Energy Conversion*, 26.3 (2011): 822-830.G.